BEILSTEIN JOURNAL OF ORGANIC CHEMISTRY

Circularly polarized luminescent systems fabricated by Tröger's base derivatives through two different strategies

Cheng Qian[‡1], Yuan Chen[‡1], Qian Zhao[1], Ming Cheng[1], Chen Lin[1], Juli Jiang[*1] and Leyong Wang[*1,2]

Letter

Open Access

Address:
[1]Key Laboratory of Mesoscopic Chemistry of MOE, Jiangsu Key Laboratory of Advanced Organic Materials, School of Chemistry and Chemical Engineering, Nanjing University, Nanjing, 210023, China and [2]Advanced Materials Institute, Qilu University of Technology (Shandong Academy of Sciences), Jinan, 250014, China

Email:
Juli Jiang[*] - jjl@nju.edu.cn; Leyong Wang[*] - lywang@nju.edu.cn

* Corresponding author ‡ Equal contributors

Keywords:
circularly polarized luminescence; chiral resolution; co-gelation; inversion of CPL handedness; Tröger's base

Beilstein J. Org. Chem. **2021,** *17,* 52–57.
https://doi.org/10.3762/bjoc.17.6

Received: 01 October 2020
Accepted: 09 December 2020
Published: 06 January 2021

This article is part of the thematic issue "Molecular recognition" and is dedicated to the memory of Carsten Schmuck.

Guest Editor: J. Niemeyer

Abstract

The Tröger's base derivative *rac*-**TBPP** was synthesized and separated into two enantiomers R_{2N}-**TBPP** and S_{2N}-**TBPP** by chiral column chromatography. These compounds show a strong circularly polarized luminescence with g_{lum} values of +0.0021, and −0.0025, respectively. The second way to fabricate the *rac*-**TBPP**-based CPL-active material is to co-gel the fluorescent *rac*-**TBPP** with a chiral D-glutamic acid gelator **DGG** by co-assembly strategy. At the molar ratio of *rac*-**TBPP**/**DGG** = 1:80, the g_{lum} value of the co-gel was about three times higher than the g_{lum} values of R_{2N}-**TBPP** and S_{2N}-**TBPP** enantiomers. Interestingly, the CPL handedness of the *rac*-**TBPP**/**DGG** co-gel could be adjusted effectively by changing their stoichiometric ratios.

Introduction

Recently, much effort has been devoted to constructing luminescent materials with efficient high emission in the solid state [1-3]. More and more types of fluorophores with aggregation-induced emission (AIE) characteristics have been discovered and applied in practice [4-6]. Among them, the fluorescent materials emitting circularly polarized luminescence (CPL) have attracted intensive interest owing to their wide applications in various researching fields including 3D displays, chiroptical materials, and so on [7-10]. Circular dichroism (CD) absorption spectra reflect the chirality of the fluorescent materials in the ground state, and circularly polarized luminescence (CPL) spectra reflect the chirality of fluorescent materials in the excited electronic state. Therefore, the CD and CPL spectrum are the two most important tools to test the chirality of luminescent materials [11,12].

As a useful building block in constructing functional materials [13,14], Tröger's base (TB), first synthesized in 1887 [15], shows high controllability and obvious advantages. There are eleven sites in its framework that could be modified without

considering the side chain. At the same time, the loose stacking of the TB unit and its derivatives, which is caused by its V-configuration could reduce the distance-dependent intermolecular quenching effect in the aggregation state [16]. Moreover, the large dihedral angle of TB (80–104°) [15] permits less self-absorption and a wider stokes shift [17]. Further, the steric hindrance and highly rigidity could reduce non-radiative transition and restrict the internal rotation [18]. More importantly, in the TB structure, its bridged methylene groups of the diazocine chiral nitrogen atoms prevent the inversion of the configuration, and two stable enantiomers could be formed and separated then. Although the TB shows excellent performance in constructing AIE materials, TB-based materials emitting CPL have rarely been reported so far. In general, the luminescent part and the chiral part are necessary to construct CPL-active materials [19-21], so the fluorescent Tröger's base derivatives *rac*-**TBPP** fall into our sight as the candidate to construct CPL-active materials. Herein, we take two stratgies to construct *rac*-**TBPP**-based CPL material. One stratgy is to separate non-CPL emission *rac*-**TBPP** into CPL-active enantiomers R_{2N}-**TBPP** and S_{2N}-**TBPP**, respectively. The other stratgy is to co-assemble the fluorescent *rac*-**TBPP** with the chiral D-glutamic acid gelator **DGG** to form the CPL-active co-gel. Interestingly, adjusting the stoichiometric ratios of *rac*-**TBPP**/**DGG** of the co-assembling system, the handedness of CPL-active co-gel can be controlled effectively (Scheme 1).

Results and Discussion

The synthetic routes of *rac*-**TBPP** are outlined in Supporting Information File 1, Scheme S1. Firstly, 2,8-dibromo-6*H*,12*H*-5,11-methanodibenzo[*b*,*f*][1,5]diazocine was synthesized according to the reported procedure [22]. Then, by Suzuki coupling reaction between 2,8-dibromo-6*H*,12*H*-5,11-methanodibenzo[*b*,*f*][1,5]diazocine and 4-vinylpyridine, *rac*-**TBPP** was successfully obtained in 51.8% yield. Detailed experiments and characterization were described in Supporting Information File 1 (Figures S1–S3). Firstly, *rac*-**TBPP** was separated into two fractions R_{2N}-**TBPP** and S_{2N}-**TBPP** by a chiralpak IB column using MeOH/DCM (80:20, v/v) as the eluent (Supporting Information File 1, Figure S5). The CD spectrum of the first fraction exhibited a positive Cotton effect at 352 nm, assigned to R_{2N}-**TBPP**, while the second one showed a negative Cotton effect at the same wavelength, assigned to S_{2N}-**TBPP** (Figure 1a) [23]. R_{2N}-**TBPP** and S_{2N}-**TBPP** were tested further by CPL spectroscopy, and the magnitude of the CPL emission was estimated by a luminescence dissymmetry factor (g_{lum}), defined as $2(I_L - I_R)/(I_L + I_R)$ where I_L and I_R are the intensity of the left-handed and right-handed CPL signals [24], respectively. Ranging from +2 for an ideal left-handed CPL to −2 for an ideal right-handed CPL, the g_{lum} value comes up to zero when no circular polarization of the luminescence was detected. The calculated value of g_{lum} of the CPL signals for R_{2N}-**TBPP** and S_{2N}-**TBPP** are +0.0021, and −0.0025, repectively (Figure 1b), which is larger than many small organic molecules [25].

In order to avoid a tedious chiral separation of *rac*-**TBPP**, we tried to construct the CPL-active material by co-assembling the achiral fluorophore *rac*-**TBPP** with a chiral gelator **DGG**. In the CPL-active co-gels, noncovalent weak interactions might be

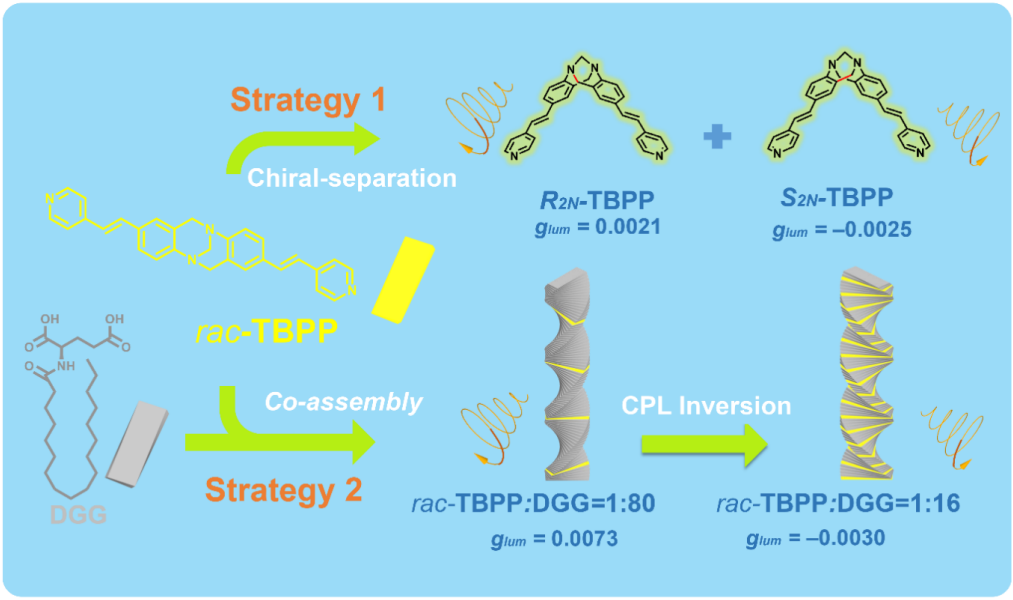

Scheme 1: Cartoon representative for *rac*-**TBPP**-based CPL-active systems fabricated through two strategies.

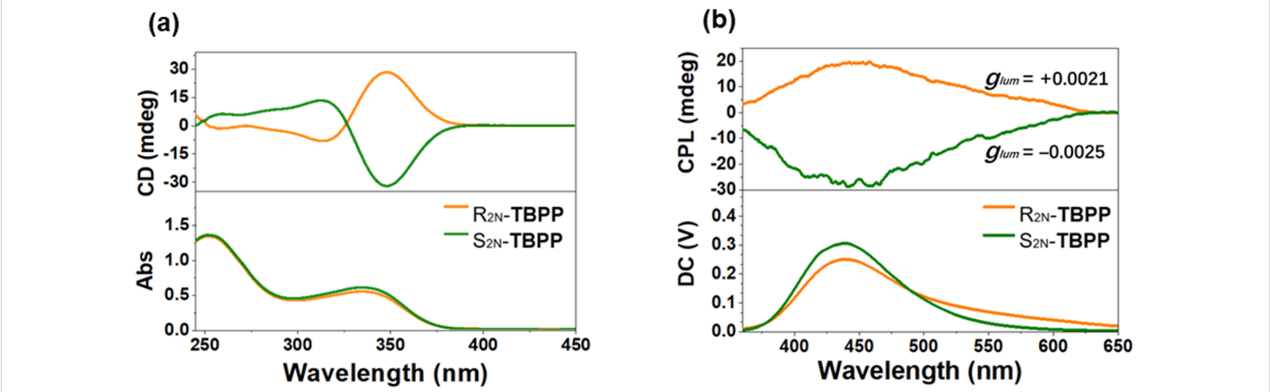

Figure 1: Ground-state and excited-state chirality of R_{2N}-**TBPP** and S_{2N}-**TBPP**. (a) CD spectra of R_{2N}-**TBPP** and S_{2N}-**TBPP**. (b) CPL spectra of R_{2N}-**TBPP** and S_{2N}-**TBPP** excited at 350 nm.

formed between achiral fluorophores and a chiral gelator. So, the CPL emission of co-gels could be adjusted easily by external stimuli. The D-glutamic acid gelator **DGG** and its enantiomer **LGG** possess three hydrogen-bond sites, two carboxylic acid groups and one amide, which could be assemblied into the stable spiral structure by hydrogen-bond and other noncovlant interactions. **DGG** was synthesised by introducing an octadecyl moiety into the glutamic skeleton in 78.6% yield according to the reported route (Supporting Information File 1, Scheme S2) [26]. When *rac*-**TBPP** was mixed with **DGG** at molar ratios from 1:100 to 1:16 (*rac*-**TBPP**/**DGG**), transparent yellow co-gels were successfully formed by being heated to dissolve in chloroform, and then cooled to ambient temperature (Supporting Information File 1, Figure S6). Owing to the AIE effect of the TB unit the fluorescence intensity of these co-assembly co-gels enhanced sharply (Figure 2a). More interestingly, at the molar ratio of *rac*-**TBPP**/**DGG** = 1:16, the CPL spectra of the co-gel shows a negative signal, while at the molar ratio of *rac*-

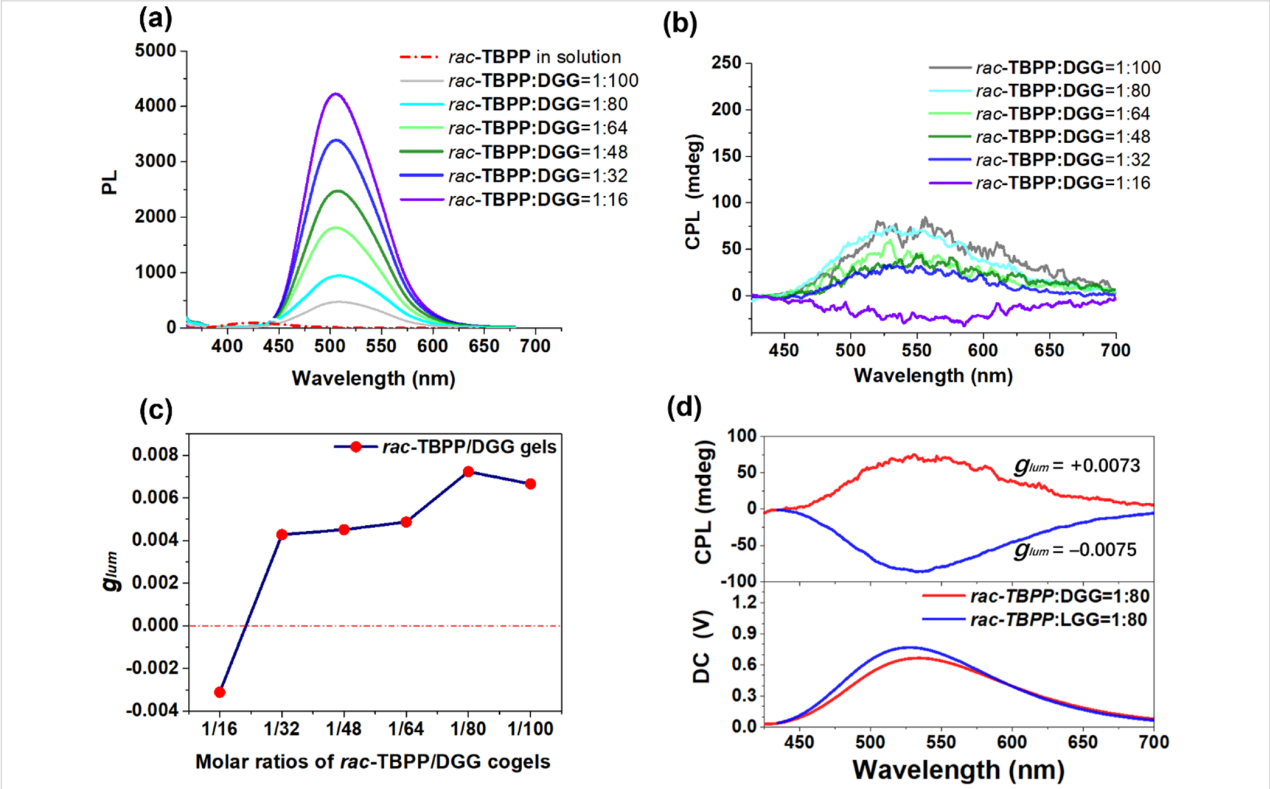

Figure 2: (a) Fluorescence spectra of *rac*-**TBPP** in solution (dash line) and in the *rac*-**TBPP**/**DGG** co-gels. (b) CPL spectra of the *rac*-**TBPP**/**DGG** co-gel at molar ratios from 1:100 to 1:16. (c) Plot of g_{lum} value of CPL signals versus ratios of *rac*-**TBPP**/**DGG** in the co-gel. (d) Mirror symmetry in CPL spectra of *rac*-**TBPP**/**DGG** co-gel (red line) and *rac*-**TBPP**/**LGG** (blue line) co-gel at the molar ratio of 1:80.

TBPP/DGG = 1:32 or higher, positive signals exhibiting left-handed CPL signals were observed (Figure 2b). At the molar ratio of *rac*-**TBPP/DGG** = 1:80, the CPL spectra shows a positive signal with a g_{lum} value about +0.0073, which was almost three times higher than the g_{lum} value of **TBPP** enantiomers (Figure 2c). Compared with the co-gel at the molar ratio of *rac*-**TBPP/DGG** = 1:80, a mirror symmetry was observed in the CPL spectra of the co-gel at the molar ratio of *rac*-**TBPP/LGG** = 1:80 (Figure 2d).

rac-**TBPP** contains pyridine units, and the gelator **DGG** has the carboxyl groups. Therefore, hydrogen bonds might be formed between pyridine in *rac*-**TBPP** and the carboxyl groups in **DGG**. Moreover, the morphologies of *rac*-**TBPP/DGG** co-gels might be different due to the changing stoichiometric ratios. In order to get an indepth understanding on the inversion of CPL handedness, *rac*-**TBPP/DGG** co-gels at molar ratios of 1:16 and 1:80 were explored further by UV–vis and FTIR (fourier transform infrared) spectra. UV–vis absorption spectra of *rac*-**TBPP/DGG** co-gels exhibited a strong absorption band at 333 nm, assigned to the conjugated structure of benzene and pyridine in the *rac*-**TBPP** (Figure 3a). However, a red-shift broaden absorption band situated at 372 nm appears in the *rac*-**TBPP/DGG** co-gel, implying the formation of the ordered packing of *rac*-**TBPP** in supramolecular assemblies. At the molar ratio of *rac*-**TBPP/DGG** = 1:80, The FTIR spectrum was similar to that of the **DGG** gel, in which $\nu_{C=O}$ bonds at 1729, 1691, and 1645 cm^{-1} reveal that the carboxyl acid groups of **DGG** could be involved in the formation of various hydrogen bonds (Figure 3b, Figure S7, Supporting Information File 1). At the molar ratio of *rac*-**TBPP/DGG** = 1:16, the intensity of the peak at 1691 cm^{-1} decreases, and the peak at 1729 cm^{-1} brodens. A new peak adjacent to 1645 cm^{-1} appears at 1627 cm^{-1}. The results demonstrate that some of the acid–acid hydrogen bonds between **DGG** molecules might be replaced by acid–pyridine hydrogen bonds between DGG and *rac*-**TBPP** [27]. In addition, the possible influence of the stoichiometric ratios to the morphologies of *rac*-**TBPP/DGG** co-gels was investigated using a scanning electron microscope (SEM). At the molar ratio of *rac*-**TBPP/DGG** = 1:80, the co-gel shows belt-like nanofibers (Figure 3c), while the fibrous morphology could not be observed at the molar ratio of 1:16 (Figure 3d). It indi-

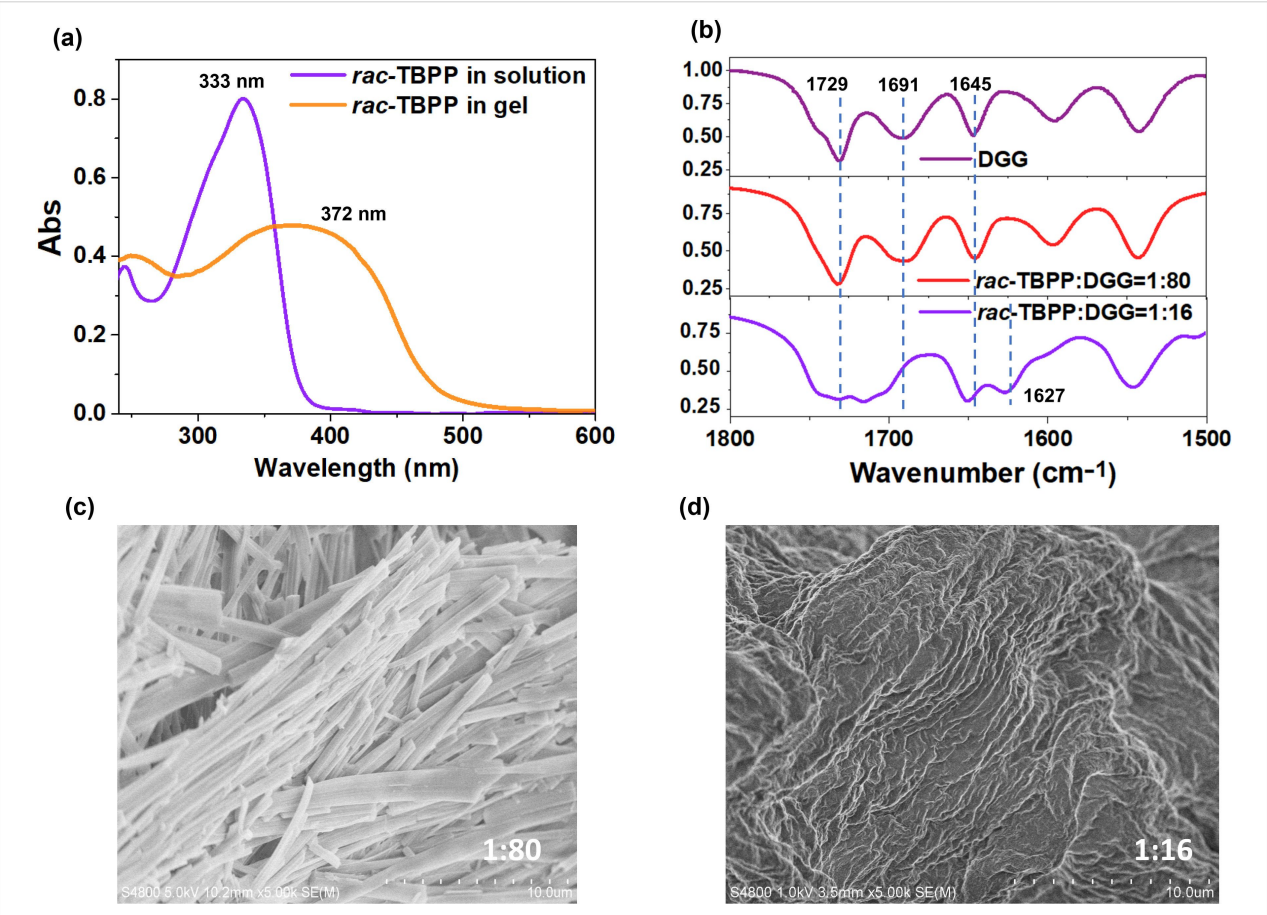

Figure 3: (a) UV–vis absorption spectra of *rac*-**TBPP** and *rac*-**TBPP/DGG** co-gel (*rac*-**TBPP/DGG** = 1:80). (b) FTIR spectra of **DGG** and *rac*-**TBPP/DGG** co-gels at molar ratios of 1:80 and 1:16, respectively. SEM images of *rac*-**TBPP/DGG** co-gels at molar ratios of 1:80 (c) and 1:16 (d).

cates that two different kinds of supramolecular assemblies were formed at the ratios of *rac*-**TBPP**/**DGG** 1:80 and 1:16, respectively, which is also coincident with the inversion of the CPL responses. However, more detailed studies are still needed to clarify the relations between the morphology and CPL handedness.

Conclusion

In conclusion, two strategies were demonstrated to obtain CPL-active materials based on the Tröger's base derivative *rac*-**TBPP**. One method is to separate *rac*-**TBPP** into two enantiomers R_{2N}-**TBPP** and S_{2N}-**TBPP**, which emit strong circularly polarized luminescence. The other strategy is to co-gel the fluorescent *rac*-**TBPP** with a chiral D-glutamic acid gelator **DGG** by the co-assembly strategy. The cogels show significant CPL emission and stoichiometry-controlled inversion of chirality due to the hydrogen bonding interactions and packing modes in the supramolecular co-assemblies. Owing to TB special V-shaped structure, rigid conformation, and nitrogen stereogenic centers make it and its derivatives useful building blocks to construct CPL-active materials and to develop chiral phosphorescent materials in future.

Supporting Information

Supporting Information File 1

Experimental part.
[https://www.beilstein-journals.org/bjoc/content/supplementary/1860-5397-17-6-S1.pdf]

Acknowledgements

We thank Prof. Carsten Schmuck for valuable suggestions and discussion on our researchs on molecular recognition during his visit in Nanjing Univ. in 2011 and afterwards.

Funding

This work was supported by the National Natural Science Foundation of China (Nos. 21901113, 21871135, 21871136), and the Natural Science Foundation of Jiangsu Province (No. BK20190287).

ORCID® iDs

Juli Jiang - https://orcid.org/0000-0001-5778-6380
Leyong Wang - https://orcid.org/0000-0001-5775-3714

Preprint

A non-peer-reviewed version of this article has been previously published as a preprint: https://doi.org/10.3762/bxiv.2020.112.v1

References

1. Zhang, Z.-Y.; Chen, Y.; Liu, Y. *Angew. Chem., Int. Ed.* **2019,** *58,* 6028–6032. doi:10.1002/anie.201901882
2. Chen, C.; Chi, Z.; Chong, K. C.; Batsanov, A. S.; Yang, Z.; Mao, Z.; Yang, Z.; Liu, B. *Nat. Mater.* **2020**. doi:10.1038/s41563-020-0797-2
3. Bolton, O.; Lee, K.; Kim, H.-J.; Lin, K. Y.; Kim, J. *Nat. Chem.* **2011,** *3,* 205–210. doi:10.1038/nchem.984
4. Zhao, Z.; Zhang, H.; Lam, J. W. Y.; Tang, B. Z. *Angew. Chem., Int. Ed.* **2020,** *59,* 9888–9907. doi:10.1002/anie.201916729
5. Li, J.; Wang, J.; Li, H.; Song, N.; Wang, D.; Tang, B. Z. *Chem. Soc. Rev.* **2020,** *49,* 1144–1172. doi:10.1039/c9cs00495e
6. Roose, J.; Tang, B. Z.; Wong, K. S. *Small* **2016,** *12,* 6495–6512. doi:10.1002/smll.201601455
7. Han, J.; Guo, S.; Lu, H.; Liu, S.; Zhao, Q.; Huang, W. *Adv. Opt. Mater.* **2018,** *6,* 1800538. doi:10.1002/adom.201800538
8. Zheng, H.; Li, W.; Li, W.; Wang, X.; Tang, Z.; Zhang, S. X.-A.; Xu, Y. *Adv. Mater. (Weinheim, Ger.)* **2018,** *30,* 1705948. doi:10.1002/adma.201705948
9. Nitti, A.; Pasini, D. *Adv. Mater. (Weinheim, Ger.)* **2020,** *32,* 1908021. doi:10.1002/adma.201908021
10. Han, J.; You, J.; Li, X.; Duan, P.; Liu, M. *Adv. Mater. (Weinheim, Ger.)* **2017,** *29,* 1606503. doi:10.1002/adma.201606503
11. Berova, N.; Bari, L. D.; Pescitelli, G. *Chem. Soc. Rev.* **2007,** *36,* 914–931. doi:10.1039/b515476f
12. Sánchez-Carnerero, E. M.; Agarrabeitia, A. R.; Moreno, F.; Maroto, B. L.; Muller, G.; Ortiz, M. J.; de la Moya, S. *Chem. – Eur. J.* **2015,** *21,* 13488–13500. doi:10.1002/chem.201501178
13. Rúnarsson, Ö. V.; Artacho, J.; Wärnmark, K. *Eur. J. Org. Chem.* **2012,** 7015–7041. doi:10.1002/ejoc.201201249
14. Dolenský, B.; Havlík, M.; Král, V. *Chem. Soc. Rev.* **2012,** *41,* 3839–3858. doi:10.1039/c2cs15307f
15. Tröger, J. *J. Prakt. Chem.* **1887,** *36,* 225–245. doi:10.1002/prac.18870360123
16. Yuan, C.-X.; Tao, X.-T.; Ren, Y.; Li, Y.; Yang, J.-X.; Yu, W.-T.; Wang, L.; Jiang, M.-H. *J. Phys. Chem. C* **2007,** *111,* 12811–12816. doi:10.1021/jp0711601
17. Xi, H.; Liu, Y.; Yuan, C.-X.; Li, Y.-X.; Wang, L.; Tao, X.-T.; Ma, X.-H.; Zhang, C.-F.; Hao, Y. *RSC Adv.* **2015,** *5,* 45668–45678. doi:10.1039/c5ra07912h
18. Yuan, R.; Li, M.-q.; Xu, J.-b.; Huang, S.-y.; Zhou, S.-l.; Zhang, P.; Liu, J.-j.; Wu, H. *Tetrahedron* **2016,** *72,* 4081–4084. doi:10.1016/j.tet.2016.05.042
19. Sang, Y.; Han, J.; Zhao, T.; Duan, P.; Liu, M. *Adv. Mater. (Weinheim, Ger.)* **2020,** *32,* 1900110. doi:10.1002/adma.201900110
20. Takaishi, K.; Iwachido, K.; Takehana, R.; Uchiyama, M.; Ema, T. *J. Am. Chem. Soc.* **2019,** *141,* 6185–6190. doi:10.1021/jacs.9b02582
21. Liang, J.; Guo, P.; Qin, X.; Gao, X.; Ma, K.; Zhu, X.; Jin, X.; Xu, W.; Jiang, L.; Duan, P. *ACS Nano* **2020,** *14,* 3190–3198. doi:10.1021/acsnano.9b08408
22. Yuan, C.; Zhang, Y.; Xi, H.; Tao, X. *RSC Adv.* **2017,** *7,* 55577–55581. doi:10.1039/c7ra11228a
23. Chen, Y.; Cheng, M.; Hong, B.; Zhao, Q.; Qian, C.; Jiang, J.; Li, S.; Lin, C.; Wang, L. *Front. Chem. (Lausanne, Switz.)* **2019,** *7,* 383. doi:10.3389/fchem.2019.00383
24. Riehl, J. P.; Richardson, F. S. *Chem. Rev.* **1986,** *86,* 1–16. doi:10.1021/cr00071a001
25. Ma, J.-L.; Peng, Q.; Zhao, C.-H. *Chem. – Eur. J.* **2019,** *25,* 15441–15454. doi:10.1002/chem.201903252

26. Bachl, J.; Mayr, J.; Sayago, F. J.; Cativiela, C.; Díaz Díaz, D. *Chem. Commun.* **2015,** *51,* 5294–5297. doi:10.1039/c4cc08593k
27. Li, P.; Lü, B.; Han, D.; Duan, P.; Liu, M.; Yin, M. *Chem. Commun.* **2019,** *55,* 2194–2197. doi:10.1039/c8cc08924h

License and Terms